were detected in APP expression between APP_{OSK}-Tg and double Tg mice (Fig. 1a, b) or in tau expression between tau264 and double Tg mice (Fig. 1c, d). The ratio of 3R/4R human tau was examined in alkaline phosphatase-treated TBS-extracts using tau12 antibody. Two discrete bands corresponding to 4R (upper) and 3R (lower) human tau were detected, and the ratio in double Tg mice was similar to that in the parent tau264 mice (Fig. 1e, f). However, while the lower bands were clearly stained with RD3 antibody (Suppl. Fig. 1a), the upper bands were not stained with RD4 antibody (Suppl. Fig. 1b). We confirmed that no mutation was incorporated into tau exon 10 of the transgene by sequencing genomic DNAs obtained from tau264 and double Tg mouse tails. It may be that some posttranslational modifications, such as acetylation at K280 [10], occurred in the RD4 epitope region (275–290 aa) of human tau to prevent the binding of the antibody.

Accelerated Aβ accumulation in double Tg mice

Amyloid pathology was examined by immunohistochemistry with Aβ oligomer-specific 11A1 antibody (Fig. 2, Suppl. Fig. 2). APP_{OSK}-Tg mice exhibited intraneuronal accumulation of Aβ oligomers in the hippocampal CA3 region, cerebral cortex, and to a lesser extent the hippocampal CA1 region at 8 months (Fig. 2a, b). In contrast, double Tg mice displayed intraneuronal accumulation of Aβ oligomers in the same regions at 6 months, earlier than that in the parent APP_{OSK}-Tg mice (Fig. 2a, b). Neither non-Tg nor tau264 mice showed 11A1-positive staining even at 24 months (Suppl. Fig. 2a). We confirmed that no amyloid plaque formation occurred in either APP_{OSK}-Tg or double Tg mice even at 24 months (Suppl. Fig. 2b).

The formation of Aβ oligomers was also examined by Western blot with β001 antibody. TBS- and GuHCl-extracts prepared from APP_{OSK}-Tg and double Tg mice at 6 months were compared. In 12 % gels, which were used for separation of low-n Aβ oligomers, only Aβ monomers were detected in TBS- but not GuHCl-extracts from both APP_{OSK}-Tg and double Tg mice (Suppl. Fig. 2c). The amount of Aβ monomers was slightly higher in double Tg mice than in APP_{OSK}-Tg mice. In 7 % gels, Aβ oligomers were detected around 50–60 kDa (corresponding to the 12-mer of Aβ) in GuHCl- but not TBS-extracts only from double Tg mice (Suppl. Fig. 2c, d). The result that Aβ oligomers were detected only in GuHCl-extracts is in agreement with our previous observation that Aβ oligomers in APP_{OSK}-Tg mice were detected in brain insoluble fractions at 24 months [46].

Accelerated tau phosphorylation in double Tg mice

Tau pathology was examined by immunohistochemistry with phosphorylated tau-specific PHF-1 and AT8 antibodies (Fig. 3, Suppl. Fig. 3). As reported previously [48], tau264 as well as non-Tg mice showed no pathology even at 24 months (Suppl. Fig. 3a–d). APP_{OSK}-Tg mice exhibited PHF-1-positive staining in the hippocampal mossy fibers at 8 months (Fig. 3a), but not in neuronal cell bodies even at 24 months (Suppl. Fig. 3c). These mice showed no AT8-positive signals even at 24 months (Suppl. Fig. 3b, d). In contrast, double Tg mice displayed PHF-1-positive and AT8-positive staining in the hippocampal mossy fibers at 6 months (Fig. 3a, b). Neuronal cell bodies also became AT8-positive in the hippocampal CA3 region and cerebral cortex at 6 months and in the CA1 regions at 12 months (Fig. 3b) and became PHF-1-positive in the hippocampal CA3 region and cerebral cortex at 12 months (Fig. 3a), but remained negative in the CA1 region even at 24 months (Suppl. Fig. 3c).

Tau hyperphosphorylation was also examined by Western blot with PHF-1 and AT8 antibodies. Again, TBS- and GuHCl-extracts prepared from APP_{OSK}-Tg and double Tg mice at 6 months were compared. In PHF-1 staining, double Tg mice exhibited higher levels of phosphorylated tau in both TBS- and GuHCl-extracts than APP_{OSK}-Tg mice (Suppl. Fig. 3e, f). In AT8 staining, no difference in positive signals in TBS-extracts was detected between the two mouse groups, but positive signals in GuHCl-extracts were higher in double Tg mice than APP_{OSK}-Tg mice (Suppl. Fig. 3g, h). TBS-extracts prepared from non-Tg mice also exhibited PHF-1- and AT8-positive signals, which presumably represent physiological tau phosphorylation.

Fig. 3 Accelerated abnormal phosphorylation of tau in double Tg ▶ mice. Brain sections were stained with phosphorylated tau-specific PHF-1 (**a**) and AT8 (**b**) antibodies at various ages. **a** In APP_{OSK}-Tg mice, hippocampal mossy fibers became PHF-1-positive at 8 months, but neuronal cell bodies remained negative up to 24 months (Suppl. Fig. 3c). In double Tg mice, hippocampal mossy fibers became PHF-1-positive at 6 months, and neuronal cell bodies became positive in the hippocampal CA3 region and cerebral cortex (CTX) at 12 months, but remained negative in the CA1 region up to 24 months (Suppl. Fig. 3c). **b** In double Tg mice, hippocampal mossy fibers became AT8-positive at 6 months, and neuronal cell bodies became positive in the hippocampal CA3 region and cerebral cortex at 6 months and in the CA1 region at 12 months. *Scale bar* 30 μm

Accelerated synapse loss in double Tg mice

An acceleration of the pathology in double Tg mice was also observed in the synapses. Our previous study showed that in APP_{OSK}-Tg mice, synaptic density in the hippocampal CA3 region, as assessed by immunostaining of the presynaptic marker synaptophysin, began to decrease at 8 months [46]. Thus, we compared synaptic density in the hippocampal CA3 region of the 4 groups at 6 and 12 months. At 6 months, no significant differences

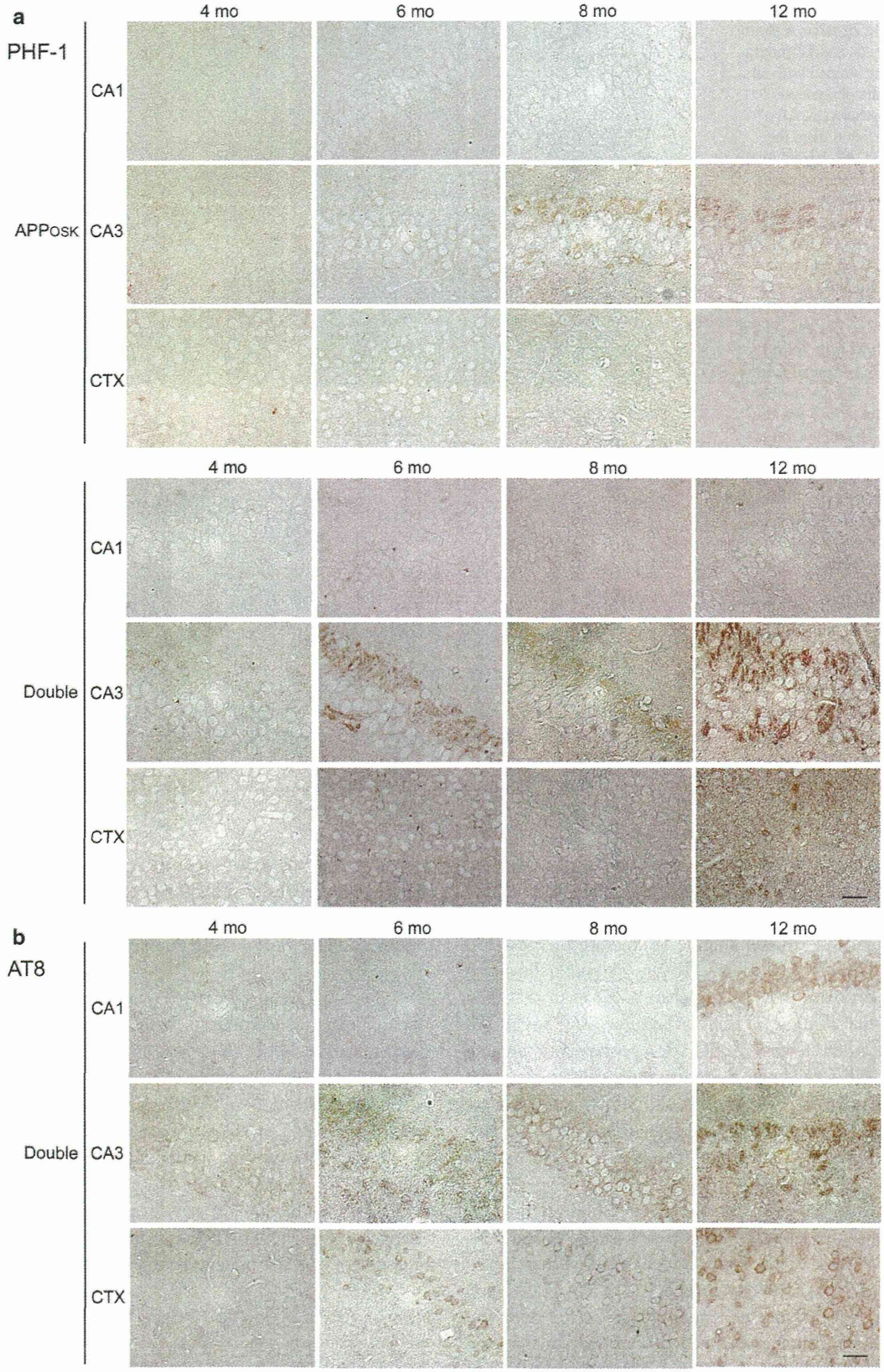
a
PHF-1
4 mo
6 mo
8 mo
12 mo
CA1
APPosk
CA3
CTX
4 mo
6 mo
8 mo
12 mo
CA1
Double
CA3
CTX
b
AT8
4 mo
6 mo
8 mo
12 mo
CA1
Double
CA3
CTX

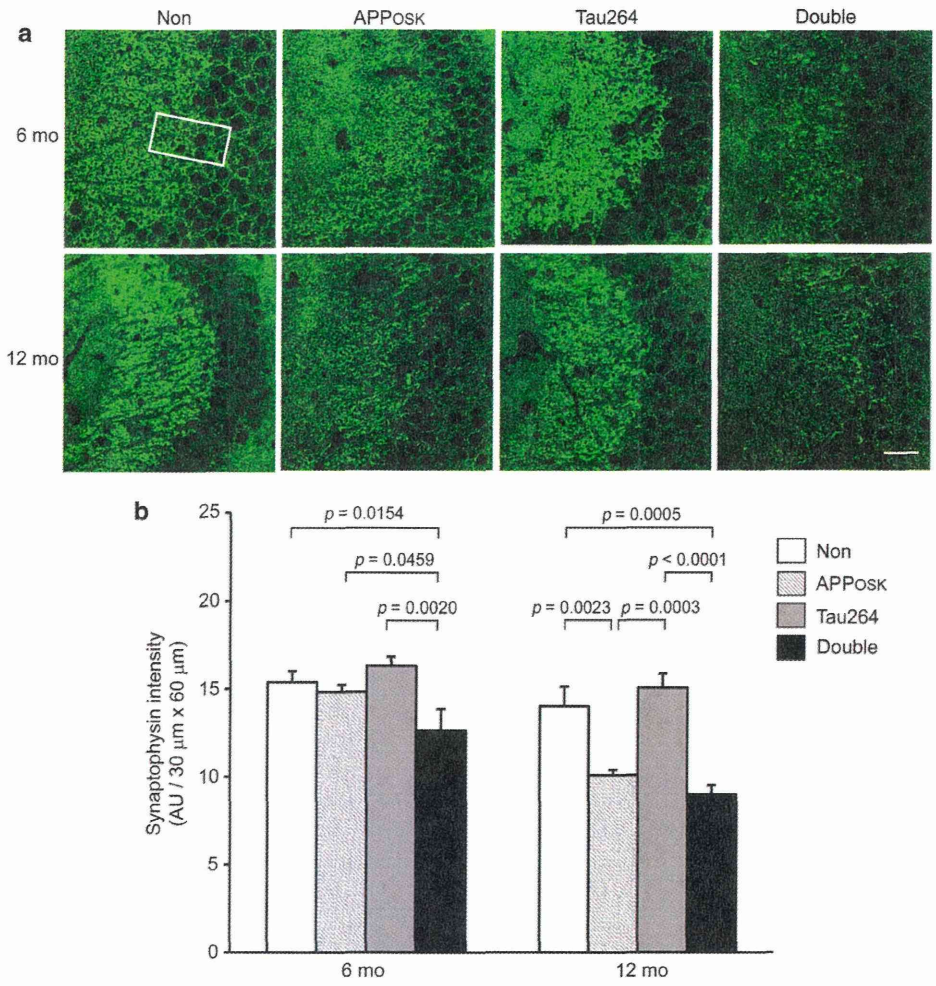

Fig. 4 Accelerated synapse loss in double Tg mice. **a** Brain sections from 6- and 12-month-old mice were stained with an antibody to the presynaptic marker synaptophysin. All images were taken from the hippocampal CA3 region. *Scale bar* 30 μm. **b** Synaptophysin fluorescence intensity in the apical dendritic-somata field (30 × 60 μm, rectangle) of the hippocampal CA3 region was quantified using NIH ImageJ software and is shown in arbitrary units (AU). Data are given as mean ± SEM ($n = 6$ for non-Tg, APP_{OSK}-Tg and tau264 at 6 months, $n = 5$ for double Tg at 6 months, $n = 5$ for non-Tg, APP_{OSK}-Tg and tau264 at 12 months, $n = 4$ for double Tg at 12 months). Double Tg mice displayed significantly lower levels of synaptophysin than the other groups at 6 months. By 12 months APP_{OSK}-Tg mice showed a significant decrease in synaptophysin levels such that they were similar to those of double Tg mice

in synaptophysin levels were observed among non-Tg, APP_{OSK}-Tg, and tau264 mice, whereas double Tg mice displayed significantly lower levels of synaptophysin (Fig. 4a, b). Synaptophysin levels in double Tg mice further lowered at 12 months, which is when APP_{OSK}-Tg mice showed a significant decrease in synaptophysin levels such that they became similar to those of double Tg mice (Fig. 4a, b). We also examined the levels of PSD-95, a postsynaptic density protein, in the same region. Again, only double Tg mice exhibited significant lower levels of PSD-95 at 6 months, and APP_{OSK}-Tg mice displayed a reduction in PSD-95 levels at 12 months to reach levels similar to those of double Tg mice (Suppl. Fig. 4a, b).

Synapse loss was also examined by Golgi staining of brain sections at 6 months. We focused on the apical dendritic-somata field of the hippocampal CA3 region, since the reduction of synaptophysin and PSD-95 was detected in this area. The number and morphology of the dendritic spines appeared unchanged in APP_{OSK}-Tg and tau264 mice compared with non-Tg mice (Suppl. Fig. 4c). In contrast, apparent loss and morphological alteration of dendritic spines were observed in double Tg mice. This observation supports the results of synaptophysin and PSD-95 stainings.

Accelerated memory loss in double Tg mice

Our previous studies revealed that cognitive function of mice declines concomitantly with synapse loss in the hippocampus [46, 48]. Thus, we assessed spatial reference memory of double Tg mice at 6 months using the Morris water maze. There were no differences in memory acquisition among non-Tg, APP_{OSK}-Tg, and tau264 mice, but double Tg mice showed significant deficits in performance, with longer escape latencies than other three groups (Fig. 5). No differences in locomotor activities were observed among all groups (not shown). These results indicate that memory impairment was also accelerated in double Tg mice.

NFT formation in double Tg mice

Our main interest is whether NFT formation occurs in the present double Tg mice, a pathology which has never

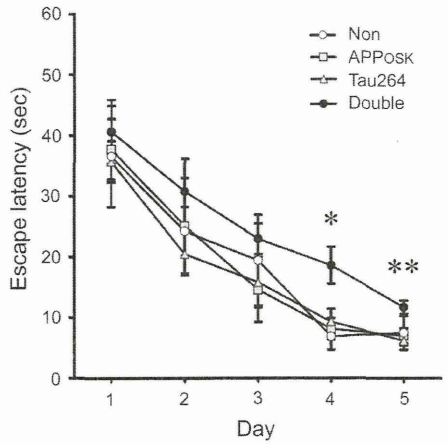

Fig. 5 Accelerated memory loss in double Tg mice. Spatial reference memory of mice was examined at 6 months using the Morris water maze. Male mice were trained to swim to a hidden platform for five consecutive days (five trials per day), and the time required to reach the platform was measured in each trial. Data are given as mean escape latency ± SEM ($n = 5$ for non-Tg, $n = 6$ for APP_{OSK}-Tg, $n = 10$ for tau264, $n = 8$ for double Tg). There were no differences in memory acquisition among non-Tg, APP_{OSK}-Tg, and tau264 mice, but double Tg mice showed significant deficits in performance, with longer escape latencies than the other three groups. *$p = 0.0051$ versus non-Tg, $p = 0.0080$ versus APP_{OSK}-Tg, $p = 0.0073$ versus tau263 at day 4; **$p = 0.0495$ versus non-Tg, $p = 0.0220$ versus APP_{OSK}-Tg, $p = 0.0032$ versus double Tg at day 5

been observed in APP-Tg mice including our APP_{OSK}-Tg mice. In Gallyas silver staining, double Tg mice displayed many positive signals within neurons in the hippocampal CA3 region and cerebral cortex, but not in the CA1 region, at 18 and 24 months (Fig. 6a). None of the other three groups showed positive signals even at 24 months (Suppl. Fig. 5a). To confirm the presence of tau filaments in the inclusions, immunoelectron microscopy with pool-2 anti-tau antibody was performed in double Tg mice. Tau-positive filamentous structures were abundantly observed within neurons in the hippocampal CA3 region and cerebral cortex at 18 and 24 months (Fig. 6b). The distribution of cytoplasmic PHF-1-positive and Gallyas-positive tau accumulation in double Tg mice paralleled that of the Aβ accumulation: dominant in the hippocampal CA3 region and cerebral cortex, and less so in the CA1 region. We noticed that this distribution was somewhat different from that of the tau pathology in our intronic mutant tau-Tg mice (lines 609 and 784), which have the same promoter and tau intronic sequences as tau264 mice: the mutant tau-Tg mice exhibited cytoplasmic PHF-1-positive and Gallyas-positive tau accumulation dominantly in the hippocampal CA1 region and cerebral cortex, and less so in the CA3 region [48]. This observation implies that NFT formation in double Tg mice was triggered by intracellular Aβ.

Whether the NFTs in double Tg mice contain both 3R and 4R tau is another issue of interest. Thus, we examined the co-localization of 3R and 4R tau at 24 months by immunohistochemistry with antibodies specific to these tau. While non-Tg and APP_{OSK}-Tg mice possessed only 4R tau, which should be endogenous mouse tau, both tau264 and double Tg mice expressed 3R tau, which presumably represents transgene-derived human tau, in addition to 4R tau (Fig. 6c, Suppl. Fig. 5b). In tau264 mice, both 3R and 4R tau were widely distributed in the hippocampal mossy fibers and neuronal cell bodies (Suppl. Fig. 5b). In contrast, double Tg mice exhibited less distribution of 4R tau in the mossy fibers and had 3R and 4R tau densely accumulate together in the neuronal cell bodies of the hippocampal CA3 region and cerebral cortex (Fig. 6c). This conclusion was confirmed by Western blot analysis for sarkosyl insoluble fractions (GuHCl-extracts) prepared from 18-month-old double Tg mice. Two discrete bands corresponding to 3R and 4R tau were detected with human tau-specific tau12 antibody after dephosphorylation of the samples (Suppl. Fig. 5c). These results indicate that the NFTs were comprised of both 3R and 4R human tau, which resembles the composition in AD.

Accelerated neuronal loss in double Tg mice

Neuronal loss, as well as senile plaques and NFTs, is a significant pathological feature of AD. In our previous study, APP_{OSK}-Tg mice displayed significant neuronal loss in the hippocampal CA3 region at 24 months, but not at 18 months or in the cerebral cortex even at 24 months [46]. Thus, we examined neuronal loss in the 4 groups at 12 and 18 months. The number of neurons positive for the mature neuron marker NeuN was counted in a constant area of the hippocampal CA3 region and cerebral cortex. In the CA3 region, no significant differences in number of NeuN-positive cells were measured among non-Tg, APP_{OSK}-Tg, and tau264 mice at 18 months, whereas double Tg mice possessed significantly fewer neurons than the other groups (Fig. 7a, b). No neuronal loss was observed at 12 months in either region (not shown) or in the cerebral cortex at 18 months (Fig. 7a, b) for all mice.

Discussion

In the present study, we generated double Tg mice expressing mutant APP and wild-type human tau to examine the role of human tau in NFT formations. While neither parent APP_{OSK}-Tg nor tau264 mice possessed NFTs even at 24 months, double Tg mice showed NFTs at 18 months. To our knowledge, the present double Tg mouse is the first mouse model of AD displaying not only Aβ accumulation,

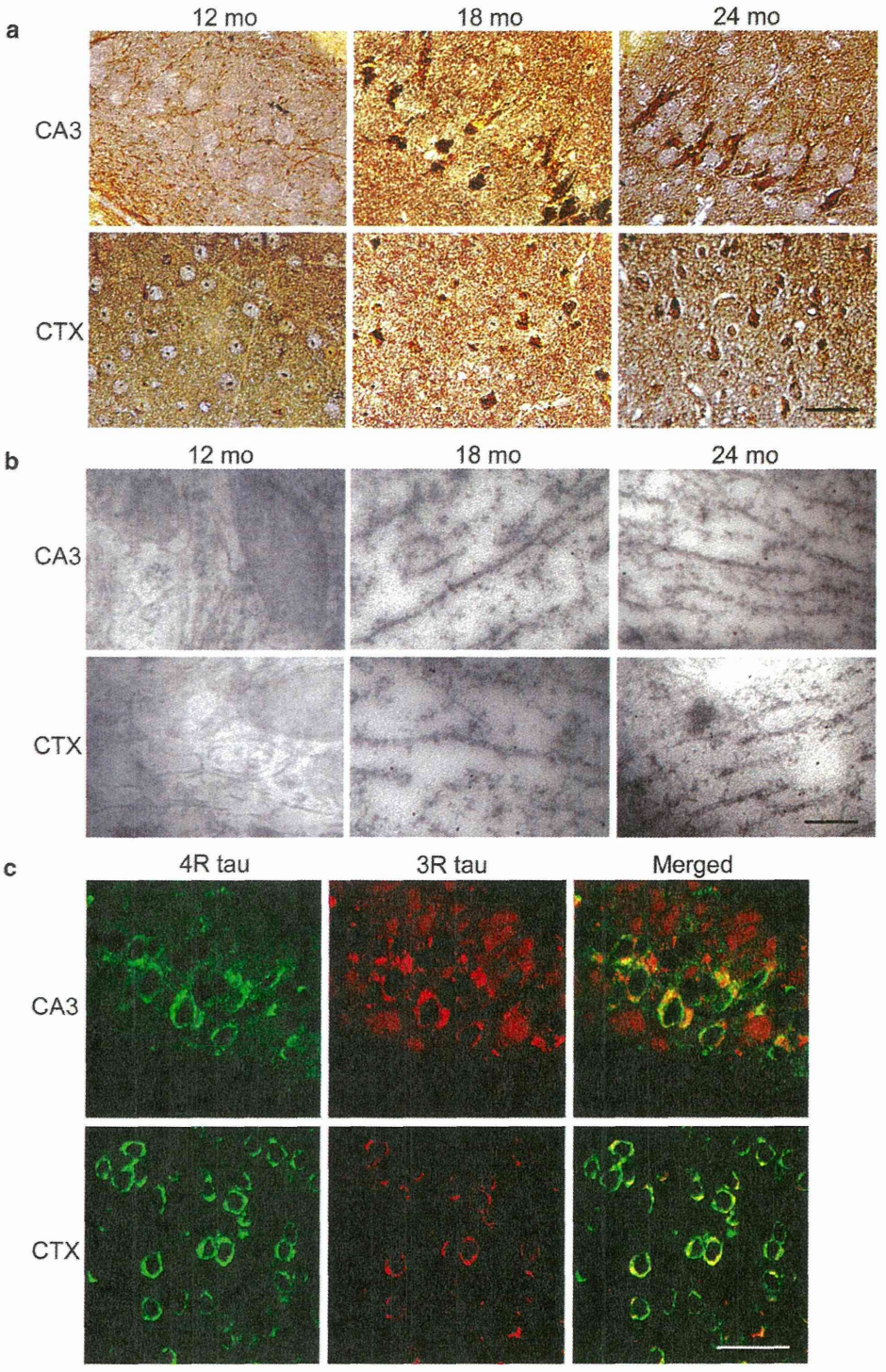

Fig. 6 NFT formation in double Tg mice. **a** Brain sections from double Tg mice were examined for NFTs by Gallyas silver staining at 12, 18, and 24 months. Many positive signals were detected at 18 and 24 months within neurons in the hippocampal CA3 region and cerebral cortex (CTX), but not the CA1 region (not shown). *Scale bar* 30 μm. **b** Brain ultrathin sections from double Tg mice were examined for tau filaments by immunoelectron microscopy with pool-2 anti-tau antibody and 10 nm gold particle-labeled second antibody at 12, 18, and 24 months. Tau-positive filamentous structures were abundantly observed within neurons in the hippocampal CA3 region and cerebral cortex at 18 and 24 months. *Scale bar* 200 nm. **c** Brain sections from 24-month-old double Tg mice were double stained with 3R tau-specific (*red*) and 4R tau-specific (*green*) antibodies. 3R and 4R tau were co-localized in neuronal cell bodies in the hippocampal CA3 region and cerebral cortex, and the distribution of 4R tau in the hippocampal mossy fibers was reduced compared with tau264 mice (Suppl. Fig. 5b). *Scale bar* 30 μm

but also NFT formation in the absence of tau mutations. It is noteworthy that these NFTs contained both 3R and 4R human tau, much like AD. This property makes the present Tg mice advantageous as a model for the investigation of the pathogenesis of AD. The distribution of cytoplasmic tau inclusions in double Tg mice paralleled Aβ accumulation, implying that NFT formation in these mice was triggered by intracellular Aβ. Our findings suggest that the presence of human tau, even at low levels (10 % of endogenous mouse tau), is critical for Aβ-induced NFT formation. Furthermore, the present Tg mice provide strong evidence that Aβ oligomers are the etiologic molecule in AD that causes

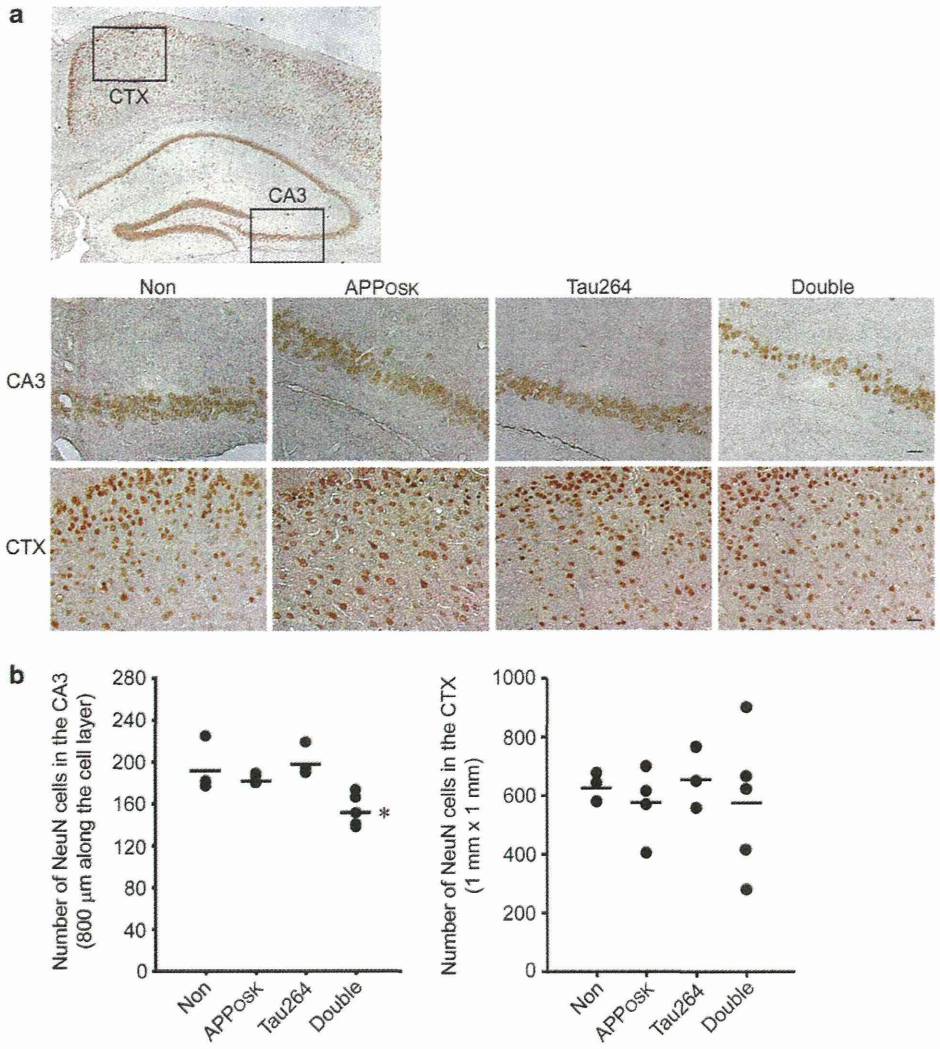

Fig. 7 Accelerated neuronal loss in double Tg mice. **a** Brain sections were stained with an antibody to the mature neuron marker NeuN at 12 and 18 months. Images of the hippocampal CA3 region (*lower rectangle* in the *top panel*) and retrosplenial region (*upper rectangle* in the *top panel*) of the cerebral cortex (CTX) at 18 months are shown. *Scale bar* 30 μm. **b** NeuN-positive cells in an area within 800 μm along the pyramidal cell layer in the hippocampal CA3 region and in an area of 1 × 1 mm in the retrosplenial region of the cerebral cortex were counted. *Dots* represent measured values for each mouse, and horizontal lines show mean values ($n = 3$ for Non-Tg and tau264, $n = 4$ for APP_{OSK}-Tg, $n = 5$ for double Tg). Double Tg mice possessed significantly fewer neurons in the hippocampus than the other groups at 18 months. $^*p = 0.0054$ versus Non-Tg, $p = 0.0175$ versus APP_{OSK}-Tg, $p = 0.0021$ versus tau264. No neuronal loss was observed at 12 months in either region (not shown) or in the cerebral cortex at 18 months for all mice

NFT formation as well as synapse and neuronal loss in the absence of amyloid plaques.

In vitro studies have shown no difference in aggregation tendency between human and mouse tau [7, 22]. Nevertheless, mouse tau appears to have a lower ability to form NFTs than human tau in vivo. Adams et al. [1] generated tau-Tg mice expressing wild-type mouse tau twofold endogenous levels by introducing the whole genome of mouse tau into the embryo. The mice developed age-dependent tau pathology, but did not show Gallyas-positive staining even at 18 months. On the other hand, Andorfer et al. [3] generated tau-Tg mice (htau mice) that express all six isoforms of wild-type human tau in the absence of endogenous mouse tau by mating genomic human tau-Tg mice (8c mice) with tau knockout mice. The expression levels of human tau in the parent 8c mice were more than threefold those of endogenous mouse tau. Despite the parent 8c mice not showing evident tau pathology, the htau mice developed intraneuronal accumulation of tau filaments at 9 months. These findings suggest that mouse tau hardly forms NFTs compared with human tau in vivo and that co-existence of mouse tau may interfere with the aggregation of human tau to prevent NFT formation. The latter hypothesis is supported by the finding that deletion of endogenous mouse tau accelerates the aggregation of human tau in mutant tau-Tg mice [2]. Therefore, NFT formation by human tau in the presence of mouse tau may require some driving forces such as tau mutations and Aβ stimulation unless human tau is massively overexpressed [19]. Once human tau starts to aggregate, it may act as a seed for the following aggregation of mouse tau. In fact, endogenous mouse tau has been shown before to aggregate together with human tau to form NFTs in mutant tau-Tg mice [33].

A noticeable difference between human and mouse tau exists in their N-terminal regions. Mouse tau lacks the 11

amino acids that correspond to the sequence from Thr17 to Gly27 in human tau. In addition, mouse tau possesses more than 30 amino acid substitutions, insertions, and deletions in comparison with human tau, many of which are in the N-terminal region. These structural differences may cause the different properties of human and mouse tau NFTs both in nature and in response to Aβ stimulation. It has been shown that tau interacts with the neural plasma membrane through its N-terminal projection domain [5] and that this interaction is negatively regulated by the phosphorylation at sites detected by PHF-1, AT8, and AT180 antibodies [29]. Microtubule binding and enrichment of tau at distal neurites are also mediated by the N-terminal projection domain, while hyperphosphorylation of tau and addition of Aβ increased the tau diffusion constant and decreased tau binding to microtubules, which may explain tau accumulation in the somatodendritic compartment of neurons [49]. These findings imply that the N-terminal region of tau plays an important role in NFT formation and that Aβ-induced tau phosphorylation affects the function of the N-terminal region. Our double Tg mice showed positive staining to both PHF-1 and AT8 antibodies and exhibited less distribution of 4R tau in the mossy fibers and instead more accumulation of 3R and 4R tau in the neuronal cell bodies than the parent tau264 mice. Phosphorylation at sites other than AT8- and PHF-1-epitopes or other modifications such as acetylation [10, 32] may also contribute to NFT formation. Overall, such modifications may be more likely in human tau than in mouse tau.

If we assume that the vulnerability of mouse tau to Aβ stimulation is lower than that of human tau, then we can explain why most APP-Tg mice failed to form NFTs. However, it has recently been shown that even rodent tau can form NFTs under certain conditions. Cohen et al. [9] generated a novel Tg rat model (TgF344-AD) expressing mutant APP and mutant presenilin 1 (PS1). Those rats expressed 2.6-fold higher human APP harboring the Swedish mutation than endogenous rat APP and 6.2-fold higher human PS1 harboring the exon 9 deletion than endogenous rat PS1, resulting in a dramatic increase in Aβ (particularly Aβ42) production. The rat further developed age-dependent amyloid and tau pathology and showed significant neuronal loss at 16 months. Notably, Gallyas-positive inclusions were detected in close proximity to the amyloid plaques at 16 months, although it is unclear whether these inclusions indeed contained tau filaments. Our APP_{OSK}-Tg mice expressed human APP at almost the same levels as endogenous mouse APP and failed to form NFTs. These findings suggest that extremely high levels of Aβ stimulation can drive endogenous rodent tau to NFT formation.

The present double Tg mice showed an accelerated accumulation of Aβ oligomers compared with parent APP_{OSK}-Tg mice. This suggests that the expression of human tau promotes Aβ production and/or aggregation or inhibits Aβ clearance. It may be that Aβ and human tau directly interact within cells. In vitro and in vivo studies have suggested that Aβ and tau form complexes that promote the aggregation of both [16, 30, 31]. In addition, the Aβ-tau complex has been shown to enhance tau phosphorylation by GSK-3β [16]. Another possibility is that human tau may affect the activities of some enzymes involved in Aβ production, such as β- and γ-secretases and GSK-3α, or Aβ degradation, such as neprilysin. In addition, co-expression of human tau with mutant Aβ may overload the capacity of cellular mechanisms (i.e., proteasomes, autophagosomes, and lysosomes) to clear misfolded proteins, leading to incomplete degradation and subsequent accumulation of both Aβ and tau. In any case, our findings suggest that Aβ and human tau synergistically interact to accelerate each other's pathology. Similar synergistic interactions have been shown in Tg mice among different amyloidogenic proteins, including Aβ, prion, tau, and α-synuclein [8, 34]. Further studies are required to elucidate the mechanism underlying these interactions.

A recent study using iPS cells derived from patients with AD suggests that AD can be classified into two categories: extracellular Aβ type and intracellular Aβ type [24]. The intracellular Aβ type neurons accumulated Aβ oligomers with molecular sizes of 50–60 kDa [24]. Our double Tg mice displayed intraneuronal accumulation of Aβ oligomers (50–60 kDa) and subsequent neuropathologies including NFT formation without forming amyloid plaques. Thus, our double Tg mice represent the intracellular Aβ type AD. However, we cannot exclude the possibility that the observed tau pathology was induced by extracellular soluble Aβ oligomers, which are more distributed than intracellular ones and, therefore, only negligibly detected by immunohistochemistry. In cultured primary neurons, exogenously added Aβ oligomers induced tau hyperphosphorylation and neurodegeneration [11, 21]. In addition, Aβ oligomer-induced synaptic alteration and neurodegeneration have been shown to be mediated by cell surface membrane receptors, such as NMDA receptors, and dendritic tau in vivo and in vitro [20, 25, 27, 43, 44]. These findings would argue that extracellular Aβ oligomers are the active species that lead to tau hyperphosphorylation and NFT formation. The extent extracellular Aβ oligomers contribute to the pathologies in our double Tg mice remains for further study.

It has been shown that human and mouse Aβ have different properties of aggregation due to their difference in amino acid sequence, with human Aβ being far more susceptible to aggregation [13]. Analogous to the possible interference between human and mouse tau, it is possible that the co-existence of mouse Aβ interferes with the aggregation of human Aβ to prevent plaque formation. This may

explain why wild-type APP-Tg mice seldom form amyloid plaques. It may be that amyloid plaque formation by human Aβ in the presence of mouse Aβ requires APP mutations to enhance Aβ production and/or aggregation and that deletion of endogenous mouse Aβ promotes plaque formation by human Aβ. If this hypothesis is true, double knockin mice expressing wild-type human APP and all six isoforms of wild-type human tau in the absence of both endogenous mouse APP and tau could display both amyloid plaques and NFTs under certain conditions, such as aging, metabolic syndromes, and stress. Such mice would be an ideal model for the investigation of the pathogenesis of sporadic AD.

Acknowledgments We thank Naomi Sakama, Reina Fujita, Maiko Mori, and Hideki Nakagawa for technical assistance, and Peter Karagiannis for reading the manuscript. This study was supported by the Grants-in-Aid for Scientific Research from the Ministry of Education, Culture, Sports, Science and Technology of Japan (no. 23110514, 24111562, 24659434, 25290018); by the Grants-in-Aid from the Ministry of Health, Labour, and Welfare, Japan; by the research funding for longevity sciences (23–39) from the National Center for Geriatrics and Gerontology, Japan; and in part by the Strategic Research Program for Brain Sciences, the Ministry of Education, Culture, Sports, Science and Technology of Japan.

Conflict of interest The authors declare that they have no conflict of interest.

References

1. Adams SJ, Crook RJ, Deture M, Randle SJ, Innes AE, Yu XZ, Lin WL, Dugger BN, McBride M, Hutton M, Dickson DW, McGowan E (2009) Overexpression of wild-type murine tau results in progressive tauopathy and neurodegeneration. Am J Pathol 175:1598–1609
2. Ando K, Leroy K, Héraud C, Yilmaz Z, Authelet M, Suain V, De Decker R, Brion JP (2011) Accelerated human mutant tau aggregation by knocking out murine tau in a transgenic mouse model. Am J Pathol 178:803–816
3. Andorfer C, Kress Y, Espinoza M, de Silva R, Tucker KL, Barde YA, Duff K, Davies P (2003) Hyperphosphorylation and aggregation of tau in mice expressing normal human tau isoforms. J Neurochem 86:582–590
4. Bolmont T, Clavaguera F, Meyer-Luehmann M, Herzig MC, Radde R, Staufenbiel M, Lewis J, Hutton M, Tolnay M, Jucker M (2007) Induction of tau pathology by intracerebral infusion of amyloid-β-containing brain extract and by amyloid-β deposition in APP × tau transgenic mice. Am J Pathol 171: 2012–2020
5. Brandt R, Léger J, Lee G (1995) Interaction of tau with the neural plasma membrane mediated by tau's amino-terminal projection domain. J Cell Biol 131:1327–1340
6. Chambers JK, Uchida K, Harada T, Tsuboi M, Sato M, Kubo M, Kawaguchi H, Miyoshi N, Tsujimoto H, Nakayama H (2012) Neurofibrillary tangles and the deposition of a beta amyloid peptide with a novel N-terminal epitope in the brains of wild Tsushima leopard cats. PLoS One 7:e46452
7. Chohan MO, Haque N, Alonso A, El-Akkad E, Grundke-Iqbal I, Grover A, Iqbal K (2005) Hyperphosphorylation-induced self assembly of murine tau: a comparison with human tau. J Neural Transm 112:1035–1047
8. Clinton LK, Blurton-Jones M, Myczek K, Trojanowski JQ, LaFerla FM (2010) Synergistic Interactions between Aβ, tau, and α-synuclein: acceleration of neuropathology and cognitive decline. J Neurosci 30:7281–7289
9. Cohen RM, Rezai-Zadeh K, Weitz TM, Rentsendorj A, Gate D, Spivak I, Bholat Y, Vasilevko V, Glabe CG, Breunig JJ, Rakic P, Davtyan H, Agadjanyan MG, Kepe V, Barrio JR, Bannykh S, Szekely CA, Pechnick RN, Town T (2013) A transgenic Alzheimer rat with plaques, tau pathology, behavioral impairment, oligomeric Aβ, and frank neuronal loss. J Neurosci 33:6245–6256
10. Cohen TJ, Guo JL, Hurtado DE, Kwong LK, Mills IP, Trojanowski JQ, Lee VM (2011) The acetylation of tau inhibits its function and promotes pathological tau aggregation. Nat Commun 2:252
11. De Felice FG, Wu D, Lambert MP, Fernandez SJ, Velasco PT, Lacor PN, Bigio EH, Jerecic J, Acton PJ, Shughrue PJ, Chen-Dodson E, Kinney GG, Klein WL (2008) Alzheimer's disease-type neuronal tau hyperphosphorylation induced by Aβ oligomers. Neurobiol Aging 29:1334–1347
12. Duyckaerts C, Potier MC, Delatour B (2008) Alzheimer disease models and human neuropathology: similarities and differences. Acta Neuropathol 115:5–38
13. Dyrks T, Dyrks E, Masters CL, Beyreuther K (1993) Amyloidogenicity of rodent and human βA4 sequences. FEBS Lett 324:231–236
14. Frank S, Clavaguera F, Tolnay M (2008) Tauopathy models and human neuropathology: similarities and differences. Acta Neuropathol 115:39–53
15. Goedert M, Spillantini MG, Cairns NJ, Crowther RA (1992) Tau proteins of Alzheimer paired helical filaments: abnormal phosphorylation of all six brain isoforms. Neuron 8:159–168
16. Guo JP, Arai T, Miklossy J, McGeer PL (2006) Aβ and tau form soluble complexes that may promote self aggregation of both into the insoluble forms observed in Alzheimer's disease. Proc Natl Acad Sci USA 103:1953–1958
17. Hardy J, Allsop D (1991) Amyloid deposition as the central event in the aetiology of Alzheimer's disease. Trends Pharmacol Sci 12:383–388
18. Hurtado DE, Molina-Porcel L, Iba M, Aboagye AK, Paul SM, Trojanowski JQ, Lee VM (2010) Aβ accelerates the spatiotemporal progression of tau pathology and augments tau amyloidosis in an Alzheimer mouse model. Am J Pathol 177:1977–1988
19. Ishihara T, Zhang B, Higuchi M, Yoshiyama Y, Trojanowski JQ, Lee VM (2001) Age-dependent induction of congophilic neurofibrillary tau inclusions in tau transgenic mice. Am J Pathol 158:555–562
20. Ittner LM, Ke YD, Delerue F, Bi M, Gladbach A, van Eersel J, Wölfing H, Chieng BC, Christie MJ, Napier IA, Eckert A, Staufenbiel M, Hardeman E, Götz J (2010) Dendritic function of tau mediates amyloid-β toxicity in Alzheimer's disease mouse models. Cell 142:387–397
21. Jin M, Shepardson N, Yang T, Chen G, Walsh D, Selkoe DJ (2011) Soluble amyloid β-protein dimers isolated from Alzheimer cortex directly induce tau hyperphosphorylation and neuritic degeneration. Proc Natl Acad Sci USA 108:5819–5824
22. Kampers T, Pangalos M, Geerts H, Wiech H, Mandelkow E (1999) Assembly of paired helical filaments from mouse tau: implications for the neurofibrillary pathology in transgenic mouse models for Alzheimer's disease. FEBS Lett 451:39–44
23. Klein WL (2013) Synaptotoxic amyloid-β oligomers: a molecular basis for the cause, diagnosis, and treatment of Alzheimer's disease? J Alzheimers Dis 33:S49–S65
24. Kondo T, Asai M, Tsukita K, Kutoku Y, Ohsawa Y, Sunada Y, Imamura K, Egawa N, Yahata N, Okita K, Takahashi K, Asaka I, Aoi T, Watanabe A, Watanabe K, Kadoya C, Nakano R, Watanabe D, Maruyama K, Hori O, Hibino S, Choshi T, Nakahata T, Hioki H, Kaneko T, Naitoh M, Yoshikawa K, Yamawaki S, Suzuki S,

Hata R, Ueno S, Seki T, Kobayashi K, Toda T, Murakami K, Irie K, Klein WL, Mori H, Asada T, Takahashi R, Iwata N, Yamanaka S, Inoue H (2013) Modeling Alzheimer's disease with iPSCs reveals stress phenotypes associated with intracellular Aβ and differential drug responsiveness. Cell Stem Cell 12:487–496

25. Lacor PN, Buniel MC, Furlow PW, Clemente AS, Velasco PT, Wood M, Viola KL, Klein WL (2007) Aβ oligomer-induced aberrations in synapse composition, shape, and density provide a molecular basis for loss of connectivity in Alzheimer's disease. J Neurosci 27:796–807
26. Lewis J, Dickson DW, Lin WL, Chisholm L, Corral A, Jones G, Yen SH, Sahara N, Skipper L, Yager D, Eckman C, Hardy J, Hutton M, McGowan E (2001) Enhanced neurofibrillary degeneration in transgenic mice expressing mutant tau and APP. Science 293:1487–1491
27. Li S, Hong S, Shepardson NE, Walsh DM, Shankar GM, Selkoe D (2009) Soluble oligomers of amyloid β protein facilitate hippocampal long-term depression by disrupting neuronal glutamate uptake. Neuron 62:788–801
28. Lippa CF, Ozawa K, Mann DM, Ishii K, Smith TW, Arawaka S, Mori H (1999) Deposition of β-amyloid subtypes 40 and 42 differentiates dementia with Lewy bodies from Alzheimer disease. Arch Neurol 56:1111–1118
29. Maas T, Eidenmüller J, Brandt R (2000) Interaction of tau with the neural membrane cortex is regulated by phosphorylation at sites that are modified in paired helical filaments. J Biol Chem 275:15733–15740
30. Manczak M, Reddy PH (2013) Abnormal interaction of oligomeric amyloid-β with phosphorylated tau: Implications to synaptic dysfunction and neuronal damage. J Alzheimers Dis 36:285–295
31. Miller Y, Ma B, Nussinov R (2011) Synergistic interactions between repeats in tau protein and Aβ amyloids may be responsible for accelerated aggregation via polymorphic states. Biochemistry 50:5172–5181
32. Min SW, Cho SH, Zhou Y, Schroeder S, Haroutunian V, Seeley WW, Huang EJ, Shen Y, Masliah E, Mukherjee C, Meyers D, Cole PA, Ott M, Gan L (2010) Acetylation of tau inhibits its degradation and contributes to tauopathy. Neuron 67:953–966
33. Mocanu MM, Nissen A, Eckermann K, Khlistunova I, Biernat J, Drexler D, Petrova O, Schönig K, Bujard H, Mandelkow E, Zhou L, Rune G, Mandelkow EM (2008) The potential for β-structure in the repeat domain of tau protein determines aggregation, synaptic decay, neuronal loss, and coassembly with endogenous tau in inducible mouse models of tauopathy. J Neurosci 28:737–748
34. Morales R, Estrada LD, Diaz-Espinoza R, Morales-Scheihing D, Jara MC, Castilla J, Soto C (2010) Molecular cross talk between misfolded proteins in animal models of Alzheimer's and prion diseases. J Neurosci 30:4528–4535
35. Oddo S, Caccamo A, Shepherd JD, Murphy MP, Golde TE, Kayed R, Metherate R, Mattson MP, Akbari Y, LaFerla FM (2003) Triple-transgenic model of Alzheimer's disease with plaques and tangles: intracellular Aβ and synaptic dysfunction. Neuron 39:409–421
36. Oikawa N, Kimura N, Yanagisawa K (2010) Alzheimer-type tau pathology in advanced aged nonhuman primate brains harboring substantial amyloid deposition. Brain Res 1315:137–149
37. Paulson JB, Ramsden M, Forster C, Sherman MA, McGowan E, Ashe KH (2008) Amyloid plaque and neurofibrillary tangle pathology in a regulatable mouse model of Alzheimer's disease. Am J Pathol 173:762–772
38. Ribé EM, Pérez M, Puig B, Gich I, Lim F, Cuadrado M, Sesma T, Catena S, Sánchez B, Nieto M, Gómez-Ramos P, Morán MA, Cabodevilla F, Samaranch L, Ortiz L, Pérez A, Ferrer I, Avila J, Gómez-Isla T (2005) Accelerated amyloid deposition, neurofibrillary degeneration and neuronal loss in double mutant APP/tau transgenic mice. Neurobiol Dis 20:814–822
39. Rosen RF, Farberg AS, Gearing M, Dooyema J, Long PM, Anderson DC, Davis-Turak J, Coppola G, Geschwind DH, Paré JF, Duong TQ, Hopkins WD, Preuss TM, Walker LC (2008) Tauopathy with paired helical filaments in an aged chimpanzee. J Comp Neurol 509:259–270
40. Schultz C, Dehghani F, Hubbard GB, Thal DR, Struckhoff G, Braak E, Braak H (2000) Filamentous tau pathology in nerve cells, astrocytes, and oligodendrocytes of aged baboons. J Neuropathol Exp Neurol 59:39–52
41. Seino Y, Kawarabayashi T, Wakasaya Y, Watanabe M, Takamura A, Yamamoto-Watanabe Y, Kurata T, Abe K, Ikeda M, Westaway D, Murakami T, Hyslop PS, Matsubara E, Shoji M (2010) Amyloid β accelerates phosphorylation of tau and neurofibrillary tangle formation in an amyloid precursor protein and tau double-transgenic mouse model. J Neurosci Res 88:3547–3554
42. Serizawa S, Chambers JK, Une Y (2012) Beta amyloid deposition and neurofibrillary tangles spontaneously occur in the brains of captive cheetahs (*Acinonyx jubatus*). Vet Pathol 49:304–312
43. Shankar GM, Bloodgood BL, Townsend M, Walsh DM, Selkoe DJ, Sabatini BL (2007) Natural oligomers of the Alzheimer amyloid-β protein induce reversible synapse loss by modulating an NMDA-type glutamate receptor-dependent signaling pathway. J Neurosci 27:2866–2875
44. Tackenberg C, Brandt R (2009) Divergent pathways mediate spine alterations and cell death induced by amyloid-β, wild-type tau, and R406W tau. J Neurosci 29:14439–14450
45. Takuma H, Arawaka S, Mori H (2003) Isoforms changes of tau protein during development in various species. Brain Res Dev Brain Res 142:121–127
46. Tomiyama T, Matsuyama S, Iso H, Umeda T, Takuma H, Ohnishi K, Ishibashi K, Teraoka R, Sakama N, Yamashita T, Nishitsuji K, Ito K, Shimada H, Lambert MP, Klein WL, Mori H (2010) A mouse model of amyloid β oligomers: their contribution to synaptic alteration, abnormal tau phosphorylation, glial activation, and neuronal loss in vivo. J Neurosci 30:4845–4856
47. Tomiyama T, Nagata T, Shimada H, Teraoka R, Fukushima A, Kanemitsu H, Takuma H, Kuwano R, Imagawa M, Ataka S, Wada Y, Yoshioka E, Nishizaki T, Watanabe Y, Mori H (2008) A new amyloid β variant favoring oligomerization in Alzheimer's-type dementia. Ann Neurol 63:377–387
48. Umeda T, Yamashita T, Kimura T, Ohnishi K, Takuma H, Ozeki T, Takashima A, Tomiyama T, Mori H (2013) Neurodegenerative disorder FTDP-17-related tau intron 10 +16C → T mutation increases tau exon 10 splicing and causes tauopathy in transgenic mice. Am J Pathol 183:211–225
49. Weissmann C, Reyher HJ, Gauthier A, Steinhoff HJ, Junge W, Brandt R (2009) Microtubule binding and trapping at the tip of neurites regulate tau motion in living neurons. Traffic 10:1655–1668